

Short Communication

Mo-Doped SnO₂ Nanoparticles: A Case Study for Selective Epoxidation of Cycloocten

Azam Anaraki Firooz*

Department of Chemistry, Faculty of Science, Shahid Rajaei Teacher Training University, P.O. Box 167855-163 Tehran, Iran.

(*) Corresponding author: a.anaraki@srttu.edu

(Received: 22 September 2016 and Accepted: 07 November 2016)

Abstract

Mo-doped SnO₂ nanoparticles were prepared using hydrothermal method. The average grain size obtained by varying calcinations temperature from 160 to 500 °C showed the different sizes. Prepared materials characterized by X-Ray diffraction (XRD) and scanning electron microscopy (SEM). Also the FTIR and the UV-Vis absorptive spectra have been carried out. Mo-doped SnO₂ nanoparticles with different sizes used as a catalyst for epoxidation of cycloocten. The result revealed that the existence of Mo species caused an increasing sensitivity on epoxidation.

Keywords: Mo doped, SnO₂, Nanoparticle, Hydrothermal, Epoxidation.

1. INTRODUCTION

The recent intense research interests in nanosized particles of metals and semiconductors have been mainly attributed to the so-called quantum size effect, i.e., the size-tunable materials properties. For semiconductor nanoparticles, this is distinctly reflected in the rather significant band gap structure that is size-sensitive, and might be manifested by the varied catalysis characteristics [1]. Metal oxide nanoparticles are interesting among the most studied materials in the last decade due to the possibilities of applications such as production of technical components for optical technology, solar cells and gas sensors [2-7]. SnO₂ is an n-type wide band gap semiconducting material with direct band gap energy of 3.6 eV and indirect band gap of 2.6 eV and also known to be in a tetragonal rutile structure [8]. To take advantage of the properties of SnO₂ nanoparticles, a number of attempts have been made by developing the effective

synthetic techniques in the preparation of SnO₂ nanoparticles [9]. Doping of different metals to this material caused an increasing in the application of them. Such as, nanoparticles of SnO₂ doped with boron and indium showed a dramatic drop in the capacity of lithium batteries with the increase of dopant of B or In [10]. Also, when SnO₂ was doped with Al₂O₃, the best electrochemical performance of lithium anode cells was achieved for 10% Al-containing tin oxides [11]. Doping of WO₃ and MoO₃ on SnO₂ increases the acid catalysts properties [12]. Tin oxide nanostructures have been synthesized by a variety of techniques, including vapor transport [13], carbothermal reduction [14], laser ablation of pure tin in an oxidizing Ar/O₂ atmosphere [15], oxidation of electrodeposited tin wires [16], oxidation of tin vapors at elevated temperatures [17], solvothermal synthesis [18], electrospinning [19], sol-gel method [20] and hydrothermal method [21]. The

hydrothermal method is one of the promising techniques for synthesizing of nanoparticles because of its ability to control size and morphology of nanoparticles [21]. In this paper, we reported the influence of Mo species as dopant in the catalysis behavior on the epoxidation of cycloocten. Also, the FTIR and the UV–Vis absorptive spectra of prepared samples have been investigated.

2. MATERIALS AND METHODS

All reagents purchased from Merck and used without further purification. The samples were prepared by hydrothermal method. $\text{SnCl}_2 \cdot 2\text{H}_2\text{O}$ and $(\text{NH}_4)_6(\text{Mo})_7(\text{O})_{24} \cdot 4\text{H}_2\text{O}$ were dissolved in deionized water, then NaOH solution was doped into the solution under stirring, by which a white precipitate was obtained. The precipitate was put into a Teflon-lined autoclave. The autoclave was put into an oven, and kept for some time under 160°C , and then cooled naturally to room temperature. The product was centrifuged and washed with ethanol for several times and dried in oven at 60°C . After drying, prepared materials annealed at 300 and 500°C for 2 h. The morphology of samples were determined by using scanning electron microscopy (SEM, Philips XL30 microscope, Holland). XRD patterns were recorded in ambient air using Philips Xpert X-ray powder diffraction ($\text{CuK}\alpha$, $\lambda = 1.5406 \text{ \AA}$, Holland), at scanning speed of $2^\circ/\text{min}$ from 20° to 80° (2θ). Infrared spectra was recorded on a Bruker, Equinox 55 spectrometer. Absorption spectra were measured by a UV–vis spectrophotometer (30W, UV-C, $\lambda = 253.7 \text{ nm}$, photon provides 4.89 eV, manufactured by Philips, Holland). The catalytic activity was examined by suspending 1.5 % molar ratio (0.11 mmol) catalyst in 1 ml CH_2Cl_2 and 3.65 mmol of pre-selected alkenes. Hydrogen peroxide 30 % (1 ml) was introduced to the reaction mixture. The two phase reaction systems were stirred under refluxing conditions. The substrate and reaction products were dissolved in

organic phase and catalyst was presented in water phase. The extent of alkenes conversion was monitored by sampling aliquots of organic phase of reaction mixture every half an hours and was analyzed by gas chromatograph.

3. RESULTS AND DISCUSSION

XRD was performed to determine the crystalline structures of the samples. The XRD patterns of the as-prepared Mo-doped SnO_2 ($C_{\text{Mn}} = 0.006 \text{ gr.}$ in this case) samples calcined at three different temperatures (160 , 300 , and 500°C , respectively) for 2 h are shown in Fig. 1.

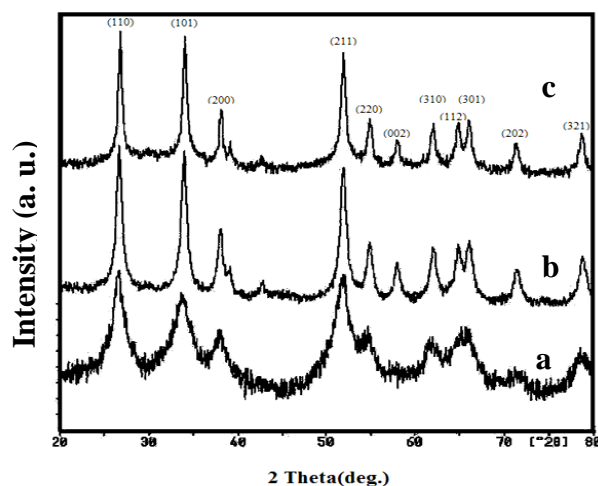


Fig.1: XRD patterns of the samples calcined at (a) 160°C (b) 300°C (c) 500°C .

The observed diffraction reflections, i.e. (110), (101), (200), (211), (220), (002), (310), (112), (301), (202) and (321) are similar to bulk SnO_2 and correspond to tetragonal rutile crystalline phases of tin oxide with standard JCPDS data card No. 41-1445. No characteristic peaks of impurities, such as molybdenum oxide or other tin oxides, were observed. The crystallite size of the prepared powders was calculated from XRD line broadening using Debye–Scherrer equation, which revealed that with increasing calcining temperature, the crystallite size gradually increased. Scanning electron microscopy (SEM) was employed to study the morphology of samples. The SEM

morphology of the nanoparticles at different temperature is shown in Fig.2.

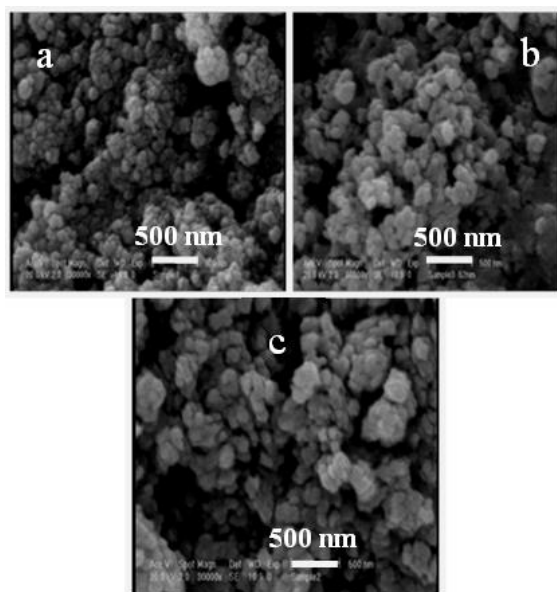


Figure 2. SEM morphology of samples calcined at (a) 160, (b) 300 (c) 500°C respectively.

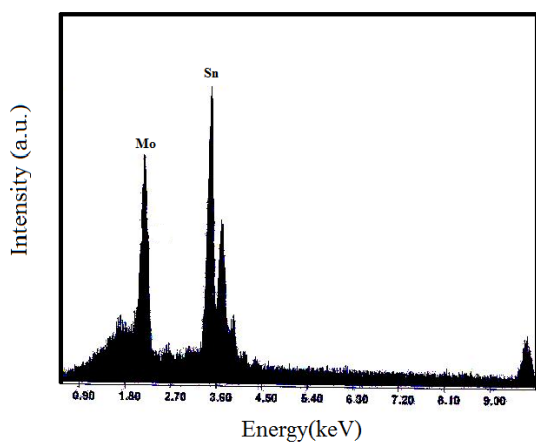


Figure 3. EDS image of Mo-doped SnO₂ nanoparticles.

When the chemical compositions of each state were analyzed by EDS, it was found that the atomic percent of Mo was about 7.49% as shown in Fig.3. Fig.4 shows the FTIR spectra of the prepared SnO₂ samples before and after calcining at 500 °C. For un-calcined state of sample, it can be seen an intense and very broad IR peak ranging from 1000 to 2000 cm⁻¹, which

may be due to absorbed water and NH₃. After calcination, this peak disappeared. Increasing calcining temperature resulted in the decrease of the intensity of the water band, and after heating at 500 °C, the bands attributed NH₃ around 3000 and 1400 cm⁻¹ disappear.

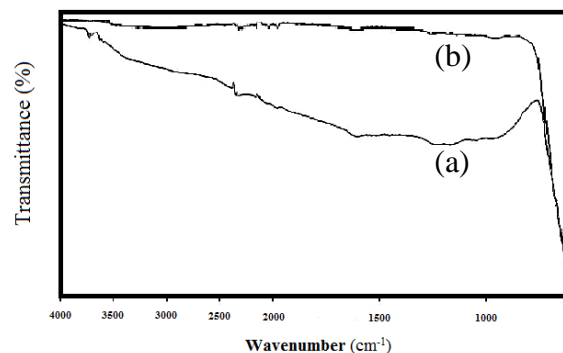


Figure 4. FTIR spectra of samples at (a) 160 (b) 500°C.

also, one intense broad band around 500 cm⁻¹ of this sample was observed. After calcining at 500 °C, the intensity of this band increased remarkably. These bands are assigned to the antisymmetric Sn–O–Sn stretching mode of the surface-bridging oxide formed by condensation of adjacent surface hydroxyl groups. The spectra changes can be easily attributed to changes in the size and the shape of the SnO₂ particles. Nanosized semiconductor particles generally exhibit threshold energy in the optical absorption measurements with decreasing particle size [22]. The optical absorption spectrum of the samples calcined at three different temperatures (160, 300, and 500 °C, respectively) are shown in Fig. 5.

It can be observed that the absorption spectra have a red shift with increasing the calcining temperature, which is consistent with the effect of quantum confinement when the semiconductor particles are in nanoscaled range.

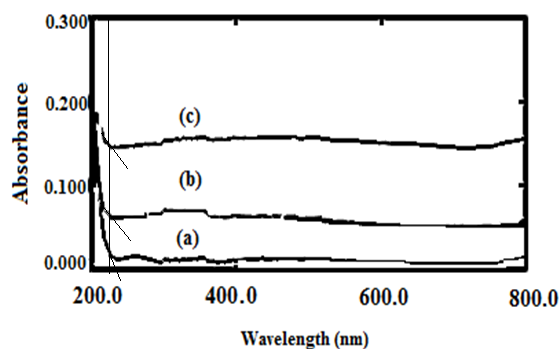


Figure 5. Optical absorption spectrum of the samples calcined at, (a) 160, (b) 300, (c) 500°C.

The catalysis test was carried out on epoxidation of cyclooctene in liquid phase, using hydrogen peroxide as an environmentally benign oxidant at room temperature. The result revealed that the existence of Mo species caused epoxydation sensitivity increment. It concluded that conversion was quite low when SnO₂ was used as a catalyst but using Mo doped SnO₂ enhanced conversion. The selectivity was 99.9 % and the conversion was 92.8 %, 89.7% and 45 % for samples calcined at 500°C, 300°C, and 160°C, respectively. Results showed that prepared catalyst could successfully catalyzed the epoxy-

dation of cyclooctene with high reactivity and selectivity. It was observed that with increasing temperature, the conversion decreased due to the more activity. In low temperature, there were many OH groups on the surface, showed in IR spectra. The developed Mo doped SnO₂ nanostructure catalyst with excellent activity may help further to design new catalyst. The details mechanistic path is under study.

4. Conclusions

We have described the synthesis of Mo doped SnO₂ catalysts at different temperatures for selective epoxidation of cyclooctene with hydrogen peroxide as an oxidant. The catalysts were characterized by XRD, FT-IR and SEM. The result revealed that the existence of Mo species caused an increasing sensitivity on epoxydation. The best catalyst is Mo doped SnO₂ synthesized at 160°C with 92.8 % conversion due to more activity with many OH groups on its surface. Therefore, it is recommended as a suitable catalyst for epoxidation of olefins.

REFERENCES

- Gu, F., Wang, S. F., Lu, M. K., Qi, Y. X., Zhou, G. J., Dong, X., Yuan, D. R. (2003). "Luminescent properties of Mn²⁺-doped SnO₂ nanoparticles", *Inorg. Chem. Commun.*, 6: 882–885.
- Anaraki Firooz, A., (2016). "A low temperature hydrothermal synthesis of ZnO doped SnO₂ nanoparticles with high photocatalytic activity" *Int. J. Nanosci. Nanotechnol.*, 12: 1-5.
- Akgul, F. A, Gumus, C. O., Er, A., Farha, A. H., Akgul, G., Ufuktepe, Y., Liu, Z. H. (2013). "Structural and electronic properties of SnO₂". *J. Alloys Comp.*, 579:50–56.
- Banisharif, A., Hakim Elahi, S., Anaraki Firooz, A., Khodadadi A. A., Mortazavi, Y. (2013). "TiO₂ /Fe₃O₄ nanocomposite photocatalysts for enhanced photo-decolorization of congo red dye" *Int. J. Nanosci. Nanotechnol.*, 9:193-202.
- Szyszkla, B., Loebmann, P., Georg, A., May, C., Elsaesser, C., (2010). "Development of new transparent conductors and device applications utilizing a multidisciplinary approach" *Thin Solid Films*, 518:3109-3114.
- Batzill, M., Diebold, U. (2005). "The surface and materials science of tin oxide" *Prog. Surf. Sci.* 79:47–154.
- Zhai, T., Fang, X., Liao, M., Xu, X., Zeng, H., Yoshio, B., Golberg, D. A., (2009). "Comprehensive Review of One-Dimensional Metal-Oxide Nanostructure Photodetectors" *Sensors*, 9: 6504-6529.
- Ikhmayies S., (2012). "Properties of Amorphous SnO₂ Thin Films, Prepared by Thermal Evaporation" *Inter. J. Mater. Chem.*, 2(4):173-177.
- Pang, G. S., Chen S., Koltypin, Y, Zaban, A., Feng, S., Gedanken, A. (2001). "Controlling the Particle Size of Calcined SnO₂ Nanocrystals" *Nanoletters*, 1 (12): 723–726.

10. Morales, J., Sanchez, L., (1999). "Electrochemical behaviour of SnO₂ doped with boron and indium in anodes for lithium secondary batteries" *Solid State Ionic*, 126:219.
11. Alcántara, R., Fernández-Madrigal F. J., Pérez-Vicente, C., Tirado, J. L., Jumas, J. C., Olivier-Fourcade, J. (2000). "Preparation. Sintering and electrochemical properties of tin dioxide and Al-doped tin dioxides obtained from citrate precursors" *Chem. Mater.*, 12:3044-3051.
12. Maksimove, G. M., Fedotov, M. A., Bogdanove, S. V., Litvask, G. S. (2000). "Synthesis and study of acid catalyst 30% WO₃/SnO₂" *J. Molec. Catal. A, chem.*;158: 435.
13. Dai, Z. R., Pan, Z. W., Wang, Z. L. (2003) "Novel nanostructures of functional oxides synthesized by thermal evaporation" *Adv. Func. Mater.*, 13: 9–24.
14. Budak S., Miao, G., Ozdemir, M., Chetry, K. B., Gupta, A. (2006). "Growth and characterization of single crystalline tin oxide (SnO₂) nanowires", *J. Cryst. Growth*, 291: 405–411.
15. Liu, Z., Zhang, D., Han, S., Li, C., Tang, T., Jin, W., Liu, X., Lei, B., Zhou, C. (2003). "Laser ablation synthesis and electron transport studies of tin oxide nanowires" *Adv. Mater.*, 15:1754-1757.
16. Kolmakov, A., Zhang, Y., Cheng, G., Moskovits, M. (2003). "Detection of CO and O₂ using tin oxide nanowire sensors. *Adv. Mater.*, 15:997–1000.
17. Ma, Y. J., Zhou, F., Lu, L., Zhang, Z. (2004). "Low-temperature transport properties of individual SnO₂ nanowires" *Solid State Communications*, 130:313–316.
18. Jiang, X., Wang, Y., Herricks, T., Xia, Y. (2004). "Ethylene glycol mediated synthesis of metal oxide nanowires" *J. of Mater. Chem.*, 14:695–703.
19. Li, D., Wang Y, Xia, Y. (2004). "Electrospinning nanofibers as uniaxially aligned arrays and layer-by-layer stacked films" *Adv. Mater.*, 16:361–366.
20. Zhang, W. F., Zhang, M. S., Yin, Z. (2000) "Microstructures and visible photoluminescence of TiO₂ nanocrystals" *Phys Status Solid (a)*, 179:319–327.
21. Yu, Q., Su-qin L., Ke-long, H., Dong, F., Xue-ying, Z., Hua-wei, H. (2012). "Hydrothermal synthesis and characterization of Eu-doped GaOOH/ α -Ga₂O₃/ β -Ga₂O₃ nanoparticles Trans.Nonferrous" *Met. Soc. China*, 20:1458-1462.
22. Saravanakumara, M., Agilan, .S, Muthukumarasamy, N., Rukkumani, V., Marusamy, A., Ranjitha, A. (2015). "Effect of Mn Doping on the Structural Optical and Magnetic Properties of SnO₂ Nanoparticles" *Acta Physica Polonica A*, 127: 1656-1661.